9

A Fully Analytic Treatment of Resonant Inductive Coupling in the Far Field

Raymond J. Sedwick
University of Maryland, College Park, Maryland, USA

1. Introduction

The principal behind Resonant Inductive Coupling (RIC) was first recognized and exploited by Tesla (Tesla, 1914), and its potential is often seen demonstrated by the operation of the eponymic Tesla coil. His work on RIC then, just as with the work of many groups now, was focused on the development of a means for wirelessly transmitting power. While Tesla's goal was much more ambitious (global transmission of power) the more modest goal of most current research is to power small electronics over a range of several meters. A resurgence of interest occurred in large part due to a an analysis (Karalis, 2007) where Coupled Mode Theory (CMT) was used to provide a framework to predict and assess the system performance over medium range distances. These distances are characterized as being large in comparison to the transmit and receive antennas, but small in comparison to the wavelength of the transmitted power. An evaluation of the various loss modes (to be discussed shortly) showed that for antennas made from standard conductors, the maximum power coupling efficiency occurs near 10 MHz, where the combination of resistive and radiative losses are at a minimum. The effective range of these systems – a few meters at non-negligible efficiencies – is adequate to power personal electronics (laptops, cell phones) or other equipment within a room.

Follow-on research (Sedwick, 2009) investigated the performance benefit that could be achieved by eliminating the ohmic losses of the coils through the use of high temperature superconducting (HTS) wire. It was shown that this allowed for the frequency to be lowered, with a corresponding reduction in radiative losses, providing an overall increase in efficiency over even 100's of meters. Because of the lower frequency, a higher self-capacitance of the coil could be tolerated allowing for a more compact "flat spiral" design, rather than the helical coil geometry used by Karalis. The ribbon geometry that is typical for HTS wire[1] is also well suited to forming such a flat spiral, and both the self-inductance and self-capacitance of the resulting structure (and therefore the resonant frequency) can be estimated analytically in the limit that the inter-turn spacing is small in comparison to the wire width. The analytic formulation of the resonant frequency from the geometry of the coil forms the basis of the current treatment.

A limitation to operating a superconducting version of RIC is the need to cryogenically cool the HTS components. This is more easily achieved on the transmit side of the system where

[1] See for instance "American Superconductor" (http://www.amsc.com/)

power is plentiful, but requires a bit of bootstrapping on the receive side, where enough power must be delivered to both supply the load and power the thermal control system. One solution is to develop a hybrid system, whereby the transmit antenna is superconducting but the receive antenna is not. The performance of such a system is expected to fall somewhere between the fully superconducting and fully non-superconducting versions, and the first part of this paper provides a model to predict this hybrid performance. The remainder of the paper then looks at the application of a hybrid RIC system to close-range communications that would be impervious to the attenuation experienced by radiative systems.

2. Extension of the performance model

The analysis of Karalis, et al. and later that of Sedwick employed CMT (Haus, 1984) as a framework for treating the system as a set of first order linear differential equations in power amplitude. Using a resonant circuit, a complex amplitude corresponding to the instantaneous power is defined

$$a = \sqrt{\frac{C}{2}}v + j\sqrt{\frac{L}{2}}i \qquad W = a^* a = \frac{C}{2}V_{\max}^2 = \frac{L}{2}I_{\max}^2 \tag{1}$$

where C,L are the capacitance and inductance, V,I are the peak voltage and current, v,i are the instantaneous voltage and current and W is the total energy contained within the circuit. With this definition, losses that are small with respect to the recirculated power are introduced using coupling parameters as

$$\begin{aligned} \dot{a}_1 &= j\omega_0 a_1 - \Gamma_1 a_1 + j\kappa_{12} a_2 \\ \dot{a}_2 &= j\omega_0 a_2 - \Gamma_2 a_2 + j\kappa_{21} a_1 - \Gamma_W a_2 \end{aligned} \tag{2}$$

where $\Gamma_1 a_1$, $\Gamma_2 a_2$ are unrecoverable drains to the environment, $\kappa_{12} a_2$, $\kappa_{21} a_1$ are each exchanges with the other resonant device and $\Gamma_W a_2$ is delivered to the load. It can be shown by energy conservation that under this definition the coupling coefficients must be equal ($\kappa_{12} = \kappa_{21} = \kappa$). While previously it was assumed that the oscillators were identical, the possibility is considered in this work that the system is composed of inhomogeneous elements. Each coil is assumed to be of similar construction, with a ribbon wire of width w and thickness t wound into a flat spiral having N turns. The spacing between consecutive turns is d, and any dielectric in the coil (to support inter-wire spacing or to force a lower resonant frequency) will have a relative dielectric constant ε_r and a loss tangent $\tan\delta$. Depending on the design details, the losses in the coil can be ohmic (R_O), radiative (R_R), and dielectric (R_D), where each loss is expressed in terms of resistance in Ohms. The functional dependencies of these losses on the design parameters are given by

$$\begin{aligned} R_O &= \rho\frac{l}{A} = \frac{4\pi^2 RN}{w}\sqrt{\rho\bar{f}} \approx 3.9\frac{RN}{\bar{w}}\sqrt{\bar{\rho}\bar{f}} && [R]=m,\ [\bar{w}]=mm \\ R_R &\approx \frac{8\pi^3}{3}\sqrt{\frac{\mu_0}{\varepsilon_0}}\left(\frac{NA}{\lambda^2}\right)^2 \approx 0.2\,(NR^2\bar{f}^2)^2 && [\bar{\rho}]=\mu Ohm-cm \\ R_D &= \frac{\tan\delta}{\omega C} = \omega L\tan\delta \approx 316\,N^2 R\,\bar{f}\tan\delta && [\bar{f}]=10^7\,Hz \end{aligned} \tag{3}$$

where the inductance of the spiral coil has been approximated as $L = 4\mu_0 RN^2$. The units of the quantities are chosen to be most representative of typical values that might be encountered in a design and result in numerical values of order unity. In the case of the dielectric losses, loss tangents will typically be in the 10^{-4} to 10^{-3} range, depending on the material. Designs with dielectrics in the coils can typically be avoided, however the presence of tuning capacitors (unless dielectricless) will require this loss mechanism to be included. In this case, only the portion of the capacitance that has the dielectric should appear and the expression in terms of inductance would require modification. In the present work, any capacitance in the system is assumed from the coil itself. The ohmic loss relationship assumes that the frequency is high enough that the skin depth, rather than the wire thickness (t) determines the current-carrying cross-section, which is typically the case.
From Eqs. (1) and (2), the rate of energy dissipation leads to a definition for Γ.

$$\frac{dW}{dt} = -2\Gamma W = -2\Gamma\left(\frac{L}{2} I_{\max}^2\right) = -\frac{I_{\max}^2}{2} R_{diss} \quad \Rightarrow \quad \Gamma = \frac{R_{diss}}{2L} \tag{4}$$

and the coupling coefficient is defined in terms of the mutual inductance (M) by

$$\kappa = \frac{\omega M}{2(L_1 L_2)^{1/2}} \approx \left(290 \frac{\sqrt{R_1 R_2}}{D}\right)^3 \bar{f} \tag{5}$$

where the number of turns in each coil is seen to cancel. The coils have been assumed axially aligned as in (Sedwick, 2009). The power coupled from the primary to the secondary coil depends on the relative magnitudes and phases of the energy recirculating through them. This can be seen by considering the rate at which energy is lost from the primary, as given by

$$\frac{d}{dt}|a_1|^2 = \dot{a}_1 a_1^* + a_1 \dot{a}_1^* = -2\Gamma|a_1|^2 - 2\kappa(a_1^R a_2^I - a_2^I a_1^R) \tag{6}$$

where $()^R, ()^I$ refer to the real and imaginary components of the complex amplitudes of each coil. This phase dependence leads to the familiar exchange of energy between weakly coupled systems as shown in Fig. 1 for a pair of un-driven resonant pendula.
In this figure, one pendulum (the Primary Oscillator) starts at a maximum energy and the other starts at zero energy. In Eq. (6), this is equivalent to $a_1^R = a_2^I$ having a maximum value and $a_1^I = a_2^R = 0$. It is important to recognize that the amplitudes refer to the black envelope lines in the figure, which oscillate at a frequency that is determined by the coupling constant (κ), rather than the blue curves, which oscillate at the resonant frequency of the system. The actual positions of both pendula at $t = 0$ are at their respective equilibrium locations (zero offset angle), however the velocity of the first pendulum is a maximum, whereas the velocity of the second pendulum is zero. After a quarter period, all of the energy has been transferred to the second pendulum, except for that which has been lost by dissipation (Γ). Energy then flows back to the first pendulum over the next quarter period.
Without loss of generality, we will always choose this phase relationship, and we will consider the steady-state situation where power is continuously supplied to the primary coil at the same rate that it is lost (both through dissipation and coupling to the secondary) and power is continuously coupled to the secondary coil at the same rate that it is lost (both

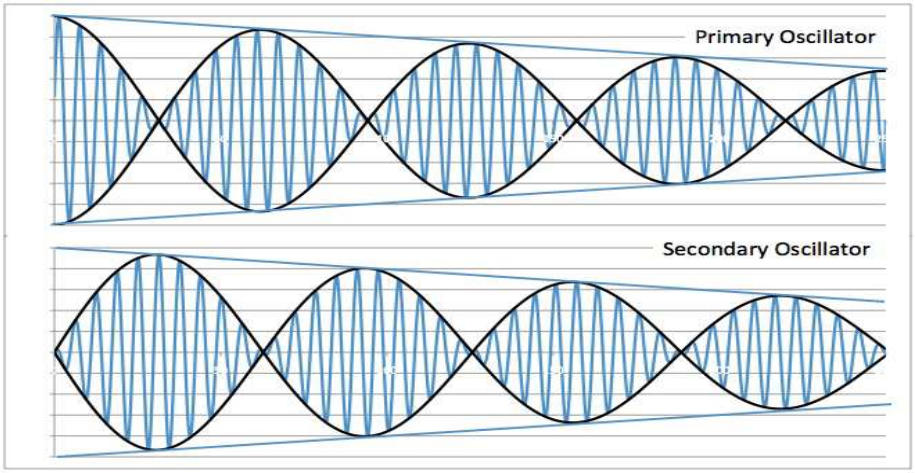

Fig. 1. Exchange of energy between two weakly coupled pendula of the same frequency.

through dissipation and driving the load). In this state, both a_1^R and a_2^I will remain constant, although not necessarily having the same value. We will also recognize that for this choice of phasing, $|a_1| = a_1^R$, $|a_2| = a_2^I$.
The steady-state condition for the secondary coil is therefore given by

$$\kappa|a_1||a_2| = (\Gamma_2 + \Gamma_W)|a_2|^2 \quad \Rightarrow \quad \omega M I_1 I_2 = (R_R + R_O + R_D + R_W) I_2^2 \tag{7}$$

the first form of which was used in (Karalis, 2007; Sedwick, 2009) to eliminate the amplitudes from the definition of the efficiency. The second form shows the relationship between the currents in the primary and secondary coils, which will generally be separation and orientation dependent as a result of the mutual inductance. The power available at the load is the difference between the coupled power and the power dissipated by the secondary coil, as illustrated in Fig. 2. Using Eq. (7) and the definitions of Eq. (1), the power to the load is given as

$$\frac{P_W}{I_2^2} = R_W = \frac{4\pi^3}{D^3}(N_1 R_1^2)(N_2 R_2^2)\left(\frac{I_1}{I_2}\right)\bar{f} - 0.2(N_2 R_2^2)^2 \bar{f}^4 - \left(\frac{4R_2 N_2 \sqrt{\bar{\rho}}}{\bar{w}}\right)\sqrt{\bar{f}} - 316 N_2^2 R_2 \tan\delta \bar{f} \tag{8}$$

where the power has been normalized by the square of the current in the secondary coil, resulting in an expression that is essentially the resistance of the load as seen by the secondary coil.

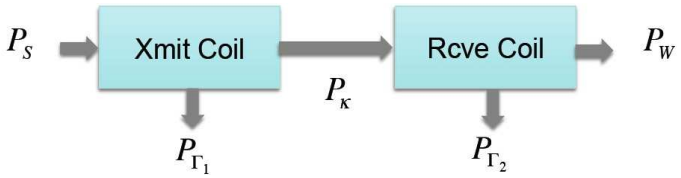

Fig. 2. Schematic of power flow from source to load showing coupling and loss paths.

Previously, an expression of this form was used to find a frequency that optimized performance, assuming that the other parameters were fixed. However, for the close-packed spiral coil (of ribbon wire) being considered here, and assuming no other reactive components are present, the natural frequency of the coil is given by (Sedwick, 2009)

$$\overline{f} \approx \frac{0.86}{R}\sqrt{\frac{\overline{d}}{\varepsilon_r N \overline{w}}} \quad \Rightarrow \quad NR^2\overline{f}^2 \approx \frac{0.75}{\varepsilon_r}\frac{\overline{d}}{\overline{w}} = \beta \tag{9}$$

where $\overline{d}, \overline{w}$ appear from the calculation of coil capacitance. For other wire geometries the parameters and numerical factors that appear on the right side may change, but the product $NR^2\overline{f}^2$ should persist, making it approximately constant from one coil to another for a given wire packing and insulation. Inserting this into Eq. (8) we find

$$\overline{I} = \frac{I_2}{I_1} = \frac{4\pi^3\beta^2}{(\overline{f}D)^3}\left[R_W + 0.2\beta^2 + \left(\frac{4\beta}{R_2\overline{w}}\right)\sqrt{\frac{\overline{\rho}}{\overline{f}^3}} + \frac{316\beta\tan\delta}{(R_2\overline{f})^3}\right]^{-1} \tag{10}$$

where the number of turns in the coil has been eliminated in lieu of the coil radius where appropriate. It is interesting to note that comparison of Eqs. (8) and (9) shows that the radiation resistance is completely specified by the details of the wire geometry and insulation. For a given primary coil current, the power delivered to the load at the secondary is then

$$P_W = \frac{I_2^2}{2}R_W = \frac{I_1^2}{2}R_W\overline{I}^2 \quad \Rightarrow \quad \overline{I}\frac{\partial\overline{I}}{\partial\overline{f}} = 0 \tag{11}$$

since the currents are given as peak values rather than RMS. Also shown is the condition that would result in a frequency that maximizes the power delivered. However, in the current form there is no longer a peak in the power delivered. Instead, the power delivered increases toward lower frequencies, corresponding to an ever-increasing number of turns, since the radius has been assumed fixed in Eq. (10). At lower frequencies the effects of dielectric and ohmic losses are seen to become problematic, leading to the dielectricless, superconducting design considered in (Sedwick, 2009). The thermal overhead of a superconducting coil in some cases may be prohibitive, but a design that avoids the use of a dielectric is critical to achieving peak performance.

Differentiating the second expression for power given in Eq. (11) with respect to the load resistance (assuming I_1 is fixed), the maximum power is delivered when the load resistance is equal to the total dissipation, a result also found in (Sedwick, 2009). This can be seen to result from the fact that while a larger load will increase power for a given current, it will also decrease the amount of current through Eq. (10). The maximum power occurs when the load is as large as possible without overly limiting the current, i.e. when it is equal to the dissipation.

2.1 Two superconducting, dielectricless coils

For the superconducting case (no ohmic or dielectric losses, and $R_W = 0.2\beta^2$), the parameter β is seen to cancel out of the current ratio, making the result independent of the wire packing and producing the same equation identified as the figure of merit (*FOM*) given in

(Karalis, 2007; Sedwick, 2009). Using Eq. (9), the maximum power delivered in the superconducting case can be expressed solely in terms of coil design parameters as

$$P_W^R \approx I_1^2 N_2^3 \left(\frac{\bar{w}}{\bar{d}}\right)\left(\frac{6.1R_2}{D}\right)^6 \tag{12}$$

where it is seen that only the secondary coil parameters are present. The geometry of the primary coil is of course constrained implicitly by Eq. (9), but this coil need not be superconducting.

For the power delivered in the non-superconducting case (but still with no dieletric), the resistive losses will dominate, and the load resistance should be matched to this quantity instead. In this case the expression for maximum power delivered is given as

$$P_W^O = I_1^2 N_2^{2.25} \left(\frac{\bar{w}}{\bar{d}}\right)^{1/4} \frac{\bar{d}}{\sqrt{\bar{\rho} R_2}} \left(\frac{3.4R_2}{D}\right)^6 \tag{13}$$

The ratio of maximum power delivered by a system with only radiative losses to one with mainly ohmic losses is then

$$\frac{P_W^R}{P_W^O} \approx 33 \frac{\sqrt{\bar{\rho} R_2}}{\bar{d}} \left(\frac{N_2 \bar{w}}{\bar{d}}\right)^{3/4} \tag{14}$$

which will typically be on the order of a few thousand. For the same power delivered, this would mean a difference in range of a factor of about 3 to 4.

To find the overall system efficiency we need to evaluate the amount of power required at the input of the primary coil. This can be found in a similar way to the power to the load in terms of the coupled power and the coil losses given by

$$\frac{P_S}{I_1^2} = \frac{P_\kappa + P_{\Gamma_1}}{I_1^2} = \frac{4\pi^3 \beta^2}{(\bar{f}D)^3}\left(\frac{I_2}{I_1}\right) + 0.2\beta^2 + \left(\frac{4\beta}{R_1 \bar{w}}\right)\sqrt{\frac{\bar{\rho}}{\bar{f}^3}} + \frac{316\beta \tan\delta}{(R_1 \bar{f})^3} \tag{15}$$

where the substitutions using Eq. (9) have already been made. As before we will first assume the case when the coil is superconducting and with no dielectric, in which case the last two terms are zero. Assuming the maximum power transfer condition, the efficiency can be written

$$\eta = \frac{P_W^R}{P_S^R} = \frac{P_\kappa - P_R}{P_\kappa + P_R} = \frac{x - \alpha \bar{I}}{x + \alpha / \bar{I}} \quad \text{where} \quad x = \frac{4\pi^3 \beta^2}{(\bar{f}D)^3},\ \bar{I} = \frac{x}{2\alpha},\ \alpha = 0.2\beta^2 \tag{16}$$

Elimination of frequency using Eq. (9) results in

$$\eta = \left[2 + 4\left(\frac{\alpha}{x}\right)^2\right]^{-1} \approx \left[2 + \left(\frac{\bar{d}}{\bar{w} N_{1,2}}\right)^3 \left(\frac{D}{9.85 R_{1,2}}\right)^6\right]^{-1} \tag{17}$$

where the number of turns and radius of either coil can be used as long as they are consistent. The radius and number of turns for either the primary or secondary coil can be

used since they must be related by the frequency matching condition. The maximum efficiency is seen to be 50% because for the maximum power transfer the load power is equal to the dissipated power in the secondary coil, and in the limit of $\alpha \to 0$ the dissipated power in the primary coil becomes negligible to that in the secondary. For a nominal coil design, with the values $\bar{w}/\bar{d} = 4, N = 100$, the efficiency drops to 10% when the coils are separated by about 280 radii.

2.2 Two non-superconducting, dielectricless coils

For the non-superconducting case, the ohmic losses will dominate the coil. We will assume at first that both the primary and the secondary are non-superconducting. The only change from Eq. (17) is the definition of α, which is now the ohmic resistance, and is unique to each coil based on its radius. This gives

$$\eta = \left[2 + 4\frac{\alpha_1\alpha_2}{x^2}\right]^{-1} \qquad \alpha_{1,2} = \left(\frac{4\beta}{R_{1,2}\bar{w}}\right)\sqrt{\frac{\bar{\rho}}{\bar{f}^3}} \tag{18}$$

Again eliminating the frequency we find

$$\eta = \left[2 + \frac{\bar{\rho}}{\bar{w}\bar{d}N_2^{1.5}}\sqrt{\frac{\bar{d}}{\bar{w}}}\frac{R_2^2}{R_1}\left(\frac{D}{3.07R_2}\right)^6\right]^{-1} \tag{19}$$

which is shown expressed in terms the secondary coil, although the radius of the primary coil does appear. Swapping all of the indices will result in the same efficiency as a result of the frequency matching condition. For two of the nominal coils as described above, with the additional information of having identical radii of 0.5 m, wire width of 4 mm and formed from copper wire, the efficiency drops to 10% when the coils are separated by 20 radii. This is a distance of just over 9 meters, as compared to 140 meters for the superconducting case.

2.3 A hybrid set of dielectricless coils

The form of the efficiency given in Eq. (18) lends itself nicely to considering hybrid system designs, since the expressions for $\alpha_{1,2}$ can refer to coils with different losses. However, remarkably the efficiency is completely symmetric with respect to which coil is the primary versus the secondary. The reason that this is unexpected is that one of the coils could have substantially more current, and one might expect that making this coil superconducting would result in a more efficient design. Let us assume that a system has a superconducting primary and a non-superconducting secondary, and that the ratio of losses is a factor of $\lambda > 1$. Swapping coils will decrease the resistance of the secondary by λ (assuming the load remains matched to the secondary losses), resulting in an increase in $\bar{I}$ by this same factor. Assuming the same power to the load, the current in the secondary must increase by a factor of $\sqrt{\lambda}$, which means that the current in the primary must be reduced by this same factor to keep the coupled power constant. The resistance of the primary is now larger by a factor of λ (the resistive coil), so the power dissipated in the primary remains the same. If the load power and dissipated powers all remain the same, so does the efficiency.

The advantage of this is that a superconducting coil can be introduced on either side of the system and will have the same effect of increasing the system efficiency. Since the

superconducting coil will have some thermal management overhead that will require power (a power which has not been accounted) it would be more useful to put it at the end of the system that is transmitting the power, where power is plentiful. However, in the case of using the system for communications (which is discussed next), both sources would have their own power supply and signals could be transmitted bi-directionally. If one of the systems has an ample supply of power, whereas the other has a limited supply of power, the superconducting coil can be placed at the power rich side for the benefit of both ends.
As a final consideration in this section, the efficiency of a hybrid system is given as

$$\eta = \left[2 + 4\frac{\alpha_1\alpha_2}{x^2}\right]^{-1} \approx \left[2 + \left(\frac{\bar{d}}{\bar{w}}\right)^{1.25} \frac{\sqrt{\bar{\rho}R_2}}{\bar{w}N_2^{2.25}} \left(\frac{D}{5.50R_2}\right)^6\right]^{-1} \tag{20}$$

For a hybrid system with the parameters specified above, the efficiency drops to 10% at a distance of 75 radii, which is the geometric mean of the distances for the other two cases as might be expected. Again the efficiency is expressed in terms of the secondary coil parameters, but can be expressed in terms of the primary by changing all of the indices.

3. Application to communications

While the efficiency drops off rapidly, one application that does not require an efficient transfer of power is communications. For example, if a receiver requires a microwatt of power to get a signal, but the transmitter is operating at only one Watt of power, the efficiency is 10^{-6}, but the system works as desired. Thus far, coupled mode analysis has been used to assess the power transfer and efficiency between resonant coils of similar designs with potentially different loss characteristics. However, the only frequency present was the resonant frequency of the system. To assess the applicability of such hybrid systems for communications, an approach must be used to capture the effect of broad-spectrum coupling.
For the purpose of transmitting signals, only three coil components will be assumed: A drive coil which is non-resonant, and a pair of resonant coils, which as previously may each have different loss characteristics. Demodulation of the signal on the secondary side will be assumed to occur directly off the secondary coil since it will provide the largest voltage. The drive coil is driven at the resonant frequency of the tuned coils, but only couples strongly to the primary coil due to both its proximity and limited magnetic flux generation. The signal into the drive coil is encoded using amplitude modulated. To proceed with the analysis, a sign convention will be established whereby current traveling clockwise around a coil (as viewed from the primary to the secondary coil, assuming that they are axially aligned) is considered positive, while a counter-clockwise current is negative.
The model for all three coils is the same (see Fig. 3), with capacitive and inductive elements having series resistors to capture the various loss modes. Beginning with the secondary coil, the governing equation is given as

$$L_S\dot{I}_S + R_S I_S + \frac{1}{C_S}q_S = emf = -M_{PS}\dot{I}_P \tag{21}$$

where I_S, q_S are the current and unbalanced charge in the coil, L_S, R_S and C_S are the effective inductance, resistance and capacitance of the coil and emf is the electromotive

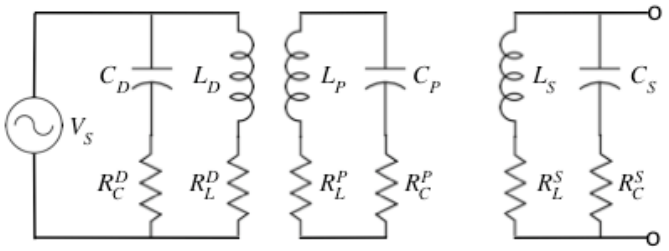

Fig. 3. Electrical model of drive, primary and secondary coils.

force induced in the secondary coil by the changing current in the primary. The resistance includes both R_C^S (dielectric loss) and R_L^S (ohmic and radiative coil losses). An increasing positive current in the primary will induce a negative *emf* in the secondary by Lentz's Law, proportional to the mutual inductance (M_{PS}) between the two coils. Differentiating with respect to time yields

$$\ddot{I}_S + 2\Gamma_S \dot{I}_S + \omega_0^2 I_S = -\frac{M_{PS}}{L_S}\ddot{I}_P \tag{22}$$

where Γ_S is the decay rate as defined previously using CMT. Similarly, the governing equation for the primary is

$$\ddot{I}_P + 2\Gamma_P \dot{I}_P + \omega_0^2 I_P = -\frac{M_{PD}}{L_P}\ddot{I}_D \tag{23}$$

where the back *emf* from the secondary has been neglected because it will be very small compared to the drive coil *emf*.

3.1 Drive coil

Treatment of the drive coil is different, since it is not driven inductively, but instead directly by an amplifier stage. It consists nominally of a single loop of wire in close proximity to the primary and has a resonant frequency that would typically be much higher than the operating frequency of the system. Current driven around the coil from the amplifier is effectively traveling through the inductive and capacitive legs in parallel, so its impedance can be found as

$$Z_D = \left(\frac{1}{R_L^D + j\omega L_D} + \frac{1}{R_C^D - j/\omega C_D}\right) = \frac{(R_L^D R_C^D + X_D^2) + jX_D(\frac{\omega}{\omega_D}R_C^D - \frac{\omega_D}{\omega}R_L^D)}{(R_L^D + R_C^D) + jX_D(\frac{\omega}{\omega_D} - \frac{\omega_D}{\omega})} \tag{24}$$

where the resistance values are as shown in Fig. 3, and X_D is the reactance of both the inductor and capacitor at the drive coil's resonant frequency (ω_D). Since this frequency is so much higher than the operating frequency of the primary and secondary coils, the impedance of the drive coil reduces to

$$Z_D = R_L^D + j\omega L_D \tag{25}$$

at all relevant frequencies. For a given applied voltage, $V_D(\omega)$, the current in the coil is simply found from Ohm's law. Assume an amplitude modulated voltage of the form

$$V_D = V_m \sin\omega_0 t\,(1+\gamma\cos\omega t) = V_m \,\mathrm{Im}[\bar{V}_D]\,, \quad \bar{V}_D = e^{j\omega_0 t} + \frac{\gamma}{2}(e^{j(\omega_0+\omega)t} + e^{j(\omega_0-\omega)t}) \tag{26}$$

where V_m is the amplitude of the carrier, γ is the amplitude of the modulation relative to the carrier, ω_0 is the carrier frequency (resonant frequency of the primary and secondary coils) and ω is the frequency of the modulation. The complex form will be used throughout the analysis for simplicity, allowing the appropriately phased solution to be found at any point by taking the imaginary component.

It should be noted that a substantial back *emf* from the primary will be seen across the drive coil, so that the voltage driving the current in the drive coil will actually be

$$V_S = V_m \bar{V}_D - M_{PD}\dot{I}_P \tag{27}$$

Knowing this, we will assume for simplicity that this back *emf* has been compensated by the amplifier, so that Eq. (26) represents V_S, the net voltage seen across the drive coil.

3.2 Primary coil

The current in the primary coil is found by solving Eq. (23), driven by V_S $(\sim V_D)$

$$\ddot{I}_P + 2\Gamma_P \dot{I}_P + \omega_0^2 I_P = -\frac{M_{PD}V_m}{L_P(R_D + j\omega L_D)}\,\ddot{\bar{V}}_D \tag{28}$$

where

$$\ddot{\bar{V}}_D = -\omega_0^2 e^{j\omega_0 t} + \frac{\gamma}{2}[-(\omega_0+\omega)^2 e^{j(\omega_0+\omega)t} - (\omega_0-\omega)^2 e^{j(\omega_0-\omega)t}] \approx -\omega_0^2 \bar{V}_D \tag{29}$$

In the last form of Eq. (29) (far right), the impact of ω versus ω_0 on the amplitude of the signal has been neglected. This is a good approximation since the modulation frequency will be small in comparison to the resonant frequency and this approximation will be made throughout the analysis. Similarly, for the current of the drive coil we will assume

$$\frac{e^{j\omega_0 t}}{R_D + j\omega_0 L_D} \approx \frac{e^{j\omega_0 t}}{j\omega_0 L_D} \quad \text{and} \quad \frac{e^{j(\omega_0 \pm \omega)t}}{R_D + j(\omega_0 \pm \omega)L_D} \approx \frac{e^{j(\omega_0 \pm \omega)t}}{j\omega_0 L_D} \tag{30}$$

where we have neglected the small relative phase shift introduced by the modulation and by the resistance of the drive coil. While the transient homogeneous solution to Eq. (28) will play a role under a continuously varying input signal, for the present analysis we are merely concerned with the frequency response of the driven system. Assuming a particular solution of the form $I_P e^{j\omega t}$, Eq. (28) becomes

$$(\omega_0^2 + 2\Gamma_P j\omega - \omega^2) I_P = -j\left(\frac{M_{PD}V_m\omega_0}{L_P L_D}\right)\bar{V}_S \tag{31}$$

Solving Eq. (31), each of the terms from $\bar{V}_S$ couple into the current of the primary as

$$\frac{e^{j\omega_0 t}}{\omega_0^2-\omega_0^2+2\Gamma_P j\omega_0} \Rightarrow \frac{-je^{j\omega_0 t}}{2\omega_0\Gamma_P},\ \frac{e^{j(\omega_0\pm\omega)t}}{\omega_0^2-(\omega_0\pm\omega)^2+2\Gamma_P j(\omega_0\pm\omega)} \Rightarrow \frac{-j(\Gamma_P\mp j\omega)e^{j(\omega_0\pm\omega)t}}{2\omega_0(\Gamma_P^2+\omega_0^2)} \quad (32)$$

and the complete expression for the current in the primary coil becomes

$$I_P = -\frac{M_{PD}V_m}{L_P L_D 2\Gamma_P}\left[e^{j\omega_0 t}+\frac{\gamma}{2}\left(c_P^* e^{j(\omega_0+\omega)t}+c_P e^{j(\omega_0-\omega)t}\right)\right],\quad c_P=\frac{\Gamma_P^2}{\Gamma_P^2+\omega_0^2}+j\frac{\omega\Gamma_P}{\Gamma_P^2+\omega_0^2} \quad (33)$$

Because of the close proximity of the drive coil to the primary, if we assume that the radii of both coils are the same, then nearly all of the flux generated by one coil will thread the other. This is equivalent to saying that the coupling coefficient (κ) is nearly unity. However in general, the mutual coupling between the drive and primary coils can be given in terms of the inductance of either coil as $M_{PD}=\kappa\sqrt{L_D L_P}=\kappa\frac{N_P}{N_D}L_D=\kappa\frac{N_D}{N_P}L_P$. Using the first expression with $N_D=1$, and substituting in for the physical definition of Γ_P, the primary current is

$$I_P = -\frac{\kappa N_P V_m}{(R_L^P+R_C^P)}\left[e^{j\omega_0 t}+\frac{\gamma}{2}\left(c_P^* e^{j(\omega_0+\omega)t}+c_P e^{j(\omega_0-\omega)t}\right)\right] \quad (34)$$

Although it may not be surprising to see the familiar Ohm's law relationship with a transformer step-up, there are two subtleties worth noting. The first is that the reactive component of the coil impedance does not appear, which is at first striking because the high Q of these coils implies that the reactive part should dominate. The second point to note is that the primary coil is not simply being driven as the "secondary" of a standard transformer, but rather at the resonance frequency of the primary. Therefore the peak voltage across the primary should well exceed the step-up resulting from simply taking the turns ratio of the transformer. These two points actually resolve themselves if we recognize that it is the reactance of the coil that actually drives it to high voltages at resonance. So, given the current found in Eq. (34), the peak voltage across the primary is not in fact $N_P V_m$, but rather $V_{peak}=I_P X_0=I_P L_p\omega_0$. The real power dissipated in the coil is however just $I_P N_P V_m$ or

$$P_{Loss}^P = \frac{(N_P V_m)^2}{R_L^P+R_C^P} = I_P^2(R_L^P+R_C^P) \quad (35)$$

While it is true that for a given drive voltage, decreasing the primary coil resistance actually increases the power dissipation, the goal is to achieve a certain level of current. Given I_P, reducing the coil resistance reduces both the power loss as well as the voltage that must be generated by the amplifier.

We can now consider the back *emf* in the drive coil that must be compensated. This is given by

$$V_D^{emf} = -M_{PD}\dot{I}_p = -\left(\kappa\frac{N_D}{N_P}L_P\right)\frac{N_P V_m j\omega_0}{(R_L^P+R_C^P)} = -j\kappa V_m\frac{L_P\omega_0}{(R_L^P+R_C^P)} = -j\kappa V_m Q_P \quad (36)$$

so that whatever the desired V_m, the back emf to be compensated will lag by 90˚ and be greater in amplitude by a factor of κQ_P, the product of the coupling constant and the quality of the primary coil.
Looking now at the complex part of the primary current, taking the imaginary component results in

$$I_P = -\frac{\kappa N_P V_m}{(R_L^P + R_C^P)} \sin\omega_0 t \left[1 + \gamma \left(\frac{\Gamma_P^2}{\Gamma_P^2 + \omega^2} \cos\omega t + \frac{\Gamma_P \omega}{\Gamma_P^2 + \omega^2} \sin\omega t \right) \right] \tag{37}$$

and in the desired low-loss limit, this becomes approximately

$$I_P = -\frac{\kappa N_P V_m}{(R_L^P + R_C^P)} \sin\omega_0 t \left[1 + \gamma \frac{\Gamma_P}{\omega} \sin\omega t \right] \tag{38}$$

where low-loss assumes that the dissipation factor is small in comparison to the modulation frequency. If we consider at what frequency the modulated signal is reduced to 50% of its original value, we find

$$\omega = 2\Gamma_P \quad \Rightarrow \quad \frac{\omega}{\omega_0} = \frac{2}{\omega_0} \frac{R_P}{2L_P} = \frac{R_P}{L_P \omega_0} = \frac{1}{Q_P} \tag{39}$$

So, as expected, the bandwidth that can be supported by the system is governed by the resonant frequency and the quality of the oscillator. To achieve both high efficiency and bandwidth, the frequency of operation should then be as high as possible. Since high frequency corresponds to radiative losses in an inductively coupled system of a given size, this sets fundamental constraints on efficiency and bandwidth. However, it also indicates that reducing the ohmic and dielectric losses in favor of radiative losses is a way to maximize bandwidth and efficiency. If it is desired to maintain low detectability, the radiated energy must be shielded in some way such as by using a Faraday cage.

3.3 Secondary coil

Continuing now to the secondary coil, the governing equation for the current is given by Eq. (22), with the driving current given by Eq. (34). As before, $\ddot{I}_S \approx -\omega_0^2 I_S$ resulting in

$$(\omega_0^2 + 2\Gamma_S j\omega - \omega^2) I_S = \frac{M_{PS}}{L_S} \omega_0^2 I_P = \frac{M_{PS}}{L_S} \frac{N_P V_m \omega_0^2}{(R_L^P + R_C^P)} \left[e^{j\omega_0 t} + \frac{\gamma}{2} \left(c_P^* e^{j(\omega_0 + \omega)t} + c_P e^{j(\omega_0 - \omega)t} \right) \right] \tag{40}$$

After similar machinations as before, the current in the secondary can be given as

$$I_S = \frac{M_{PS}}{L_S} \frac{N_P V_m \omega_0^2}{(R_L^P + R_C^P)} j e^{j\omega_0 t} \left[1 + \frac{\gamma}{2} \left(c_S^* c_P^* e^{j\omega t} + c_P^* c_P e^{-j\omega t} \right) \right], \quad c_S = \frac{\Gamma_S^2}{\Gamma_S^2 + \omega_0^2} + j \frac{\omega \Gamma_S}{\Gamma_S^2 + \omega_0^2} \tag{41}$$

Expressing the mutual inductance and self-inductances in terms of system parameters as in Section 2, the amplitude of the current in the secondary becomes

$$|I_S| = \frac{M_{PS} N_P V_m \omega_0}{2(R_L^P + R_C^P)\Gamma_S L_S} = \left(\frac{N_P^2 R_P^2}{(R_L^P + R_P^P)} \right) \left(\frac{N_S^2 R_S^2}{(R_L^S + R_C^S)} \right) \frac{4\pi^3 V_m \bar{f}}{D^3} \tag{42}$$

Dividing out the current in the primary we find

$$\frac{I_2}{I_1} = \left(\frac{N_P R_P^2 N_S R_S^2}{(R_L^S + R_C^S)}\right)\frac{4\pi^3 \bar{f}}{D^3} = \left(\frac{N_P R_P^2 N_S R_S^2}{R_W + R_{Rad}}\right)\frac{4\pi^3 \bar{f}}{D^3} =$$
$$= \left(\frac{\beta^2 / \bar{f}^4}{R_W + 0.2\beta^2}\right)\frac{4\pi^3 \bar{f}}{D^3} = \frac{4\pi^3 \beta^2}{(\bar{f}D)^3}\left[R_W + 0.2\beta^2\right]^{-1} \tag{43}$$

where we have eliminated all losses except for radiative, added in an equivalent series resistance for the load and substituted in definitions from Eqs. (3) and (9). Gratifyingly, the final expression on the right is identical to that of Eq. (10), under the same set of assumptions.
Taking only the imaginary component of Eq. (41), the current corresponding to our assumed input in the low-loss operating limit is

$$I_S = \left(\frac{N_P^2 R_P^2}{(R_L^P + R_C^P)}\right)\left(\frac{N_S R_S^2}{(R_L^S + R_C^S)}\right)\frac{4\pi^3 V_m \bar{f}}{D^3}\cos\omega_0 t\left[1 - \gamma\frac{\Gamma_P \Gamma_S}{\omega^2}\cos\omega t\right] \tag{44}$$

Considering the coefficient of the modulated waveform as before, the bandwidth based on a 50% reduction in amplitude is given by

$$\frac{\Gamma_P \Gamma_S}{\omega^2} = \frac{1}{4Q_P Q_S}\left(\frac{\omega_0}{\omega}\right)^2 = \frac{1}{2} \quad \Rightarrow \quad \Delta f = \frac{f_0}{\sqrt{2Q_P Q_S}} \tag{45}$$

and can be seen to be related to the geometric mean of the primary and secondary coil Q-factors.
As an example, we will assume an operating frequency of 10 MHz, a frequency where the radiative losses begin to be comparable to ohmic losses. Voice transmission has a bandwidth typically taken to be 4kHz[2], so the combined system Q-factor can be as high as 1800 using Eq. (45). If radiative losses are the only dissipation in the system, then the Q-factor of each coil can be calculated as

$$Q = \frac{L\omega_0}{R_{Rad}} = \frac{32\pi^2 N^2 R\bar{f}}{0.2(NR^2\bar{f}^2)^2} = \frac{160\pi^2}{(R\bar{f})^3} \Rightarrow R\bar{f} = \frac{11.6}{\sqrt[3]{Q}} \tag{46}$$

At 10 MHz, $\bar{f} = 1$, so $R = 0.95m$ from Eq. (46), but the number of turns in the coils is unspecified since both radiative resistance and reactance scale as N^2. At 1MHz, the Q-factor would need to be 10 times smaller to support the required bandwidth, requiring the coil radius to be over 21 times larger. However, there is no need to require that the dissipation be purely radiative, and only a small amount of additional dissipation is needed to substantially reduce the Q-factor.

4. Range of detection and bandwidth

For a given demodulation threshold, the ability to detect and demodulate the signal from the carrier is distance dependent by the overall strength of the received signal. The

[2] See for instance http://en.wikipedia.org/wiki/Voice_frequency

maximum voltage that will be seen across the secondary coil can be found from the current induced and the Q-factor of the coil, as was discussed with the primary coil. The modulated signal will then be attenuated as shown in Eq. (45). For the case of a superconducting secondary, these can be combined to yield

$$V_S^{\max} = I_S Q_S = I_P \left(\frac{I_S}{I_P}\right)\left(\frac{1}{4Q_P Q_S}\right)\left(\frac{\omega_0}{\omega}\right)^2 Q_S = \frac{I_P}{Q_P}\left(\frac{5\pi^3}{\overline{f}^3 D^3}\right)\left(\frac{10^7\,\overline{f}}{\Delta f}\right)^2 \approx \frac{I_P}{Q_P \overline{f}(\Delta f^*)^2}\left(\frac{2490}{D}\right)^3 \quad (47)$$

where Q_P and I_P have been left explicitly and the bandwidth (Δf^*) is in kHz. The reason is that all of the factors in the final form would be operationally derived. For instance, while an arbitrarily high primary current may be theoretically possible, power limitations or wire current capacity would most likely limit it to a maximum value. Likewise, there is no constraint on making the Q-factor of the primary large or small, so we allow it to be specified directly. The Q-factor of the secondary is seen to cancel, since while it reduces the current in the secondary it also increases the peak voltage. Although this cancellation occurs (making its value irrelevant), the relationship used for the current ratio has already assumed that only radiative losses are seen in the secondary and that the load power is negligible by comparison. In general, however, Eq. (10) can be used to find I_S / I_P for any dominant loss mode.

The achievable bandwidth and carrier frequency are not independent of the values of Q_P and Q_S, and Eq. (45) can be used to conservatively replace the carrier frequency in lieu of the Q-factors. This results in

$$V_S^{\max} \approx \frac{(10^4)\, I_P}{Q_P\sqrt{2Q_P Q_S}(\Delta f^*)^3}\left(\frac{2490}{D}\right)^3 \quad \Rightarrow \quad \Delta f^* \approx \left(\frac{I_P}{V_S^{\max} Q_P \sqrt{Q_P Q_S}}\right)^{\frac{1}{3}}\left(\frac{47800}{D}\right) \quad (48)$$

Under the present assumptions, a selection of threshold voltage, primary coil current, Q-values, and operating distance will determine the bandwidth. As an example, assume that the detection threshold is 20 mV, about four times the typical laboratory noise floor. Parallel windings of wire could allow for a recirculating primary current of 100 Amps, and quality voice communications would require $\Delta f = 4kHz \ \left(\Delta f^* = 4\right)$. High Q-factors are seen to be detrimental, however since the secondary has been assumed superconducting, the expectation is that Q_S will nevertheless be quite large – on the order of 10^6. The variation of bandwidth with distance for three values of Q_P is shown in Fig. 4.

A consequence of using a high-Q coil as a secondary is that the Q-factor of the primary must be smaller to support a given bandwidth. This translates into higher power requirements on the primary. For the case of a receiver coil that is dominated by ohmic losses, the modulated signal strength across the secondary coil is given instead by

$$V_S^{\max} = I_P \left(\frac{I_S}{I_P}\right)\left(\frac{1}{4Q_P Q_S}\right)\left(\frac{\omega_0}{\omega}\right)^2 Q_S = \frac{I_P}{Q_P}\frac{\pi^3 \beta R_2 \overline{w}}{D^3\sqrt{\overline{f}^3\overline{\rho}}}\left(\frac{10^7\,\overline{f}}{\Delta f}\right)^2 \approx \frac{I_P \beta R_2 \overline{w}}{Q_P(\Delta f^*)^2}\sqrt{\frac{\overline{f}}{\overline{\rho}}}\left(\frac{1460}{D}\right)^3 \quad (49)$$

where the ohmic term in Eq. (10) has been used for the current ratio between the secondary and the primary. Using the same substitution to eliminate the carrier frequency results in

$$V_S^{\max} \approx \frac{(Q_P Q_S)^{1/4}}{Q_P\sqrt{\bar{\rho}}} \frac{I_P \beta R_S \bar{w}}{(\Delta f^*)^{3/2}} \left(\frac{353}{D}\right)^3 \quad \Rightarrow \quad \Delta f^* \approx \left(\frac{(Q_P Q_S)^{1/4}}{Q_P\sqrt{\bar{\rho}}} \frac{I_P R_S \bar{d}}{V_S^{\max}}\right)^{\frac{2}{3}} \left(\frac{321}{D}\right)^2 \tag{50}$$

The frequency dependency now weakly favors a higher Q_S, which is now unfortunately much smaller as a result of the ohmic losses in the secondary. Using the additional assumptions of $R_S = 0.5m$, $\bar{d} = 1mm, \bar{\rho} = 1.6$ along with the same previously assumed parameters, the bandwidth is plotted as a function of distance in Fig. 5 for the same values of Q_P assumed in Fig 4.

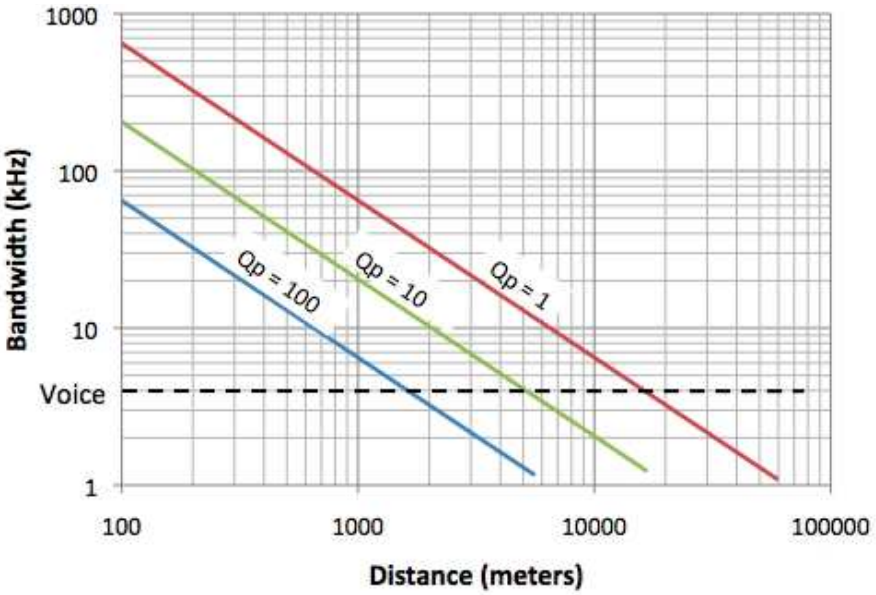

Fig. 4. Bandwidth versus distance for a superconducting secondary at different qualities.

The range is seen to be smaller overall for the ohmic loss case, and in both cases the distance is seen to increase as the Q-factor of the primary is decreased. The implication of reducing the primary Q-factor is a greater amount of power that must be expended. It should be noted that by fixing the Q-factors of the primary and secondary coils for the performance curves shown in Figs. 4 and 5, the assumed carrier frequency is changing for different values of bandwidth. These plots, therefore, do not show the reduction in bandwidth with distance of a fixed system design, but rather how the baseline design would change for different maximum ranges of operation. To see how the bandwidth of a particular system would roll off with distance would require going back to Eqs. (47) and (49).

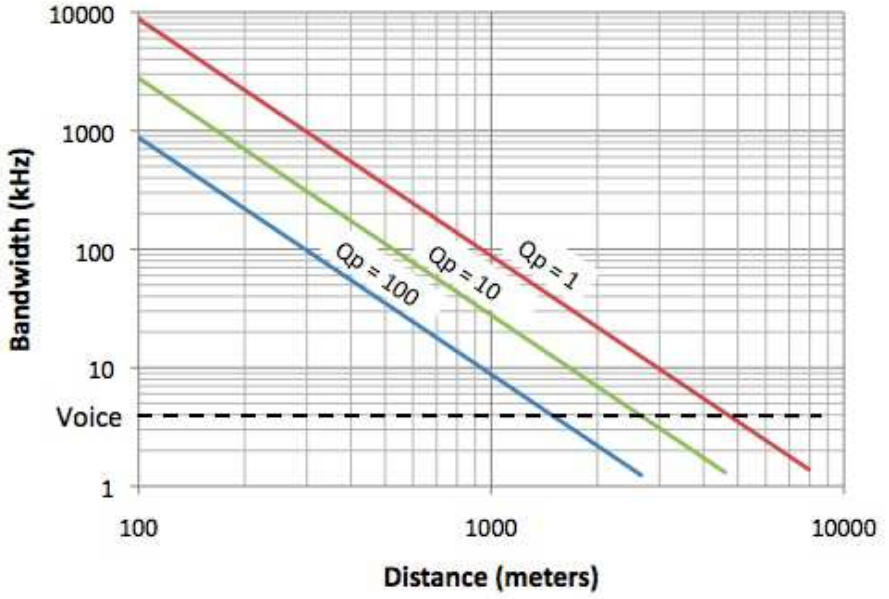

Fig. 5. Bandwidth versus distance for an ohmic secondary at different qualities.

5. Modulation

Writing the full form of Eq. (47) to include both the carrier and the modulation we find

$$V_S = I_P\left(\frac{20\pi^3}{\bar{f}^3 D^3}\right)\cos\omega_0 t\left[1-\frac{\gamma}{4}\frac{1}{Q_P Q_S}\left(\frac{\omega_0}{\omega}\right)^2\cos\omega t\right] \tag{51}$$

so that in the current example, the amplitude of the modulated signal in comparison to the DC component has a numerical value of only $8(10^{-5})$. This may make the demodulation difficult due to small variations in the carrier that could be confused with signal content.

The assumed modulation approach thus far has been a Double Sideband Full Carrier scheme (DSFC—standard AM), which has the advantage of using a simple envelope detector for demodulation. The envelope detector circuit and the resulting idealized envelope are shown in Fig. 6. Instead of transmitting a full carrier along with the signal (the unity term in Eq. (48), setting γ to a large value effectively eliminates the DC component of the modulation. This transforms the signal to a Double Sideband Suppressed Carrier (DSB-

SC) AM signal. Elimination of the carrier reduces the power required for transmission and removes variations in the carrier as a potentially competing signal. The disadvantage is that without the carrier present the signal must be mixed at the receiver with a new carrier signal that is phase-locked and frequency matched to the original. Standard methods of implementing such a system are available.

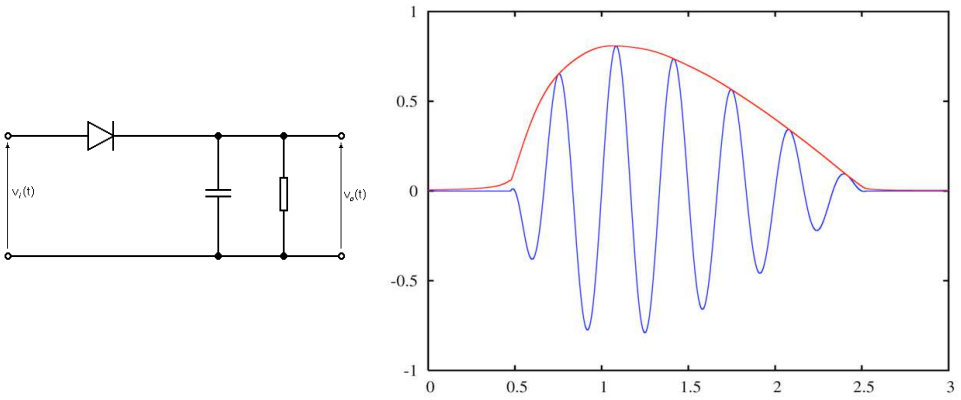

Fig. 6. Envelope detector circuit (left) and the resulting ideal envelope (right).

For communications the bandwidth is seen to roll-off with frequency for different point designs, and this reduction is demonstrated to be linear for a superconducting secondary and quadratic for a non-superconducting secondary. A large Q-factor secondary has the advantage of operating over larger distances, however the consequential need for reducing the Q-factor of the primary causes the power dissipation in the primary to be larger. Conversely, a non-superconducting secondary suffers a reduced range of operation, but levies a lower power requirement on the primary coil as a result. A system can be optimized to meet a specific bandwidth/distance requirement with the lowest power consumption.

6. Acknowledgments

The author wishes to acknowledge the support of the Defense Advanced Research Projects Agency (DARPA) Strategic Technologies Office (STO) monitored by Dr. Deborah Furey under PO No. HR0011-10-P-003. The author would also like to acknowledge Dr. Eric Prechtl of Axis Engineering Technologies, Inc. for his technical contributions to the effort.
The views expressed are those of the author and do not reflect the official policy or position of the Department of Defense or the U.S. Government. This work has been approved for Public Release, Distribution Unlimited.

7. References

Haus, H. A., Waves and Fields in Optoelectronics, Prentice-Hall, New Jersey (1984)
http://en.wikipedia.org/wiki/Voice_frequency
Karalis, A., et al., "Efficient wireless non-radiative mid-range energy transfer", Ann. Phys., 10.1016 (2007)

Sedwick, R.J.,"Long range inductive power transfer with superconducting oscillators", Ann. Phys., 325 (2010) 287–299.
Tesla, N., U.S. patent 1,119,732 (1914)

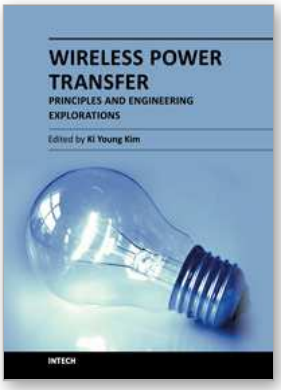

Wireless Power Transfer - Principles and Engineering Explorations
Edited by Dr. Ki Young Kim

ISBN 978-953-307-874-8
Hard cover, 272 pages
Publisher InTech
Published online 25, January, 2012
Published in print edition January, 2012

The title of this book, Wireless Power Transfer: Principles and Engineering Explorations, encompasses theory and engineering technology, which are of interest for diverse classes of wireless power transfer. This book is a collection of contemporary research and developments in the area of wireless power transfer technology. It consists of 13 chapters that focus on interesting topics of wireless power links, and several system issues in which analytical methodologies, numerical simulation techniques, measurement techniques and methods, and applicable examples are investigated.

How to reference
In order to correctly reference this scholarly work, feel free to copy and paste the following:

Raymond J. Sedwick (2012). A Fully Analytic Treatment of Resonant Inductive Coupling in the Far Field, Wireless Power Transfer - Principles and Engineering Explorations, Dr. Ki Young Kim (Ed.), ISBN: 978-953-307-874-8, InTech, Available from: http://www.intechopen.com/books/wireless-power-transfer-principles-and-engineering-explorations/a-fully-analytic-treatment-of-resonant-inductive-coupling-in-the-far-field

INTECH
open science | open minds

InTech Europe
University Campus STeP Ri
Slavka Krautzeka 83/A
51000 Rijeka, Croatia
Phone: +385 (51) 770 447
Fax: +385 (51) 686 166
www.intechopen.com

InTech China
Unit 405, Office Block, Hotel Equatorial Shanghai
No.65, Yan An Road (West), Shanghai, 200040, China
中国上海市延安西路65号上海国际贵都大饭店办公楼405单元
Phone: +86-21-62489820
Fax: +86-21-62489821